Emergent Topological Phenomena in Low-D Systems Induced by Gauge Potentials

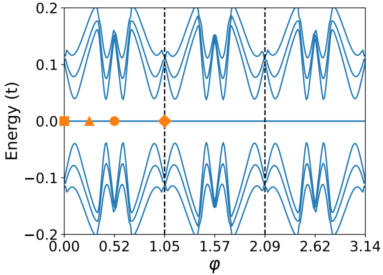

Aidan Winblad
Hua Chen

Department of Physics

Colorado State University

October 26, 2024

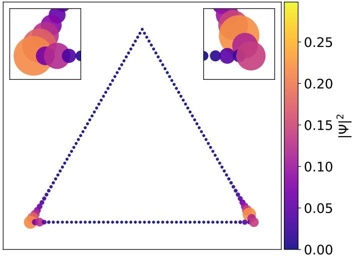

Outline

- Background:
  - Majorana fermions in particle physics and condensed matter
  - Topological states
  - Kitaev chain and Majorana number
- Motivation:
  - Braiding and topological quantum computing
  - T-junctions to triangular structures for braiding
  - Supercurrents as gauge potential
- Results: Two approaches
  - Exactly solvable miminal model
  - Hollow triangular islands & bulk-edge correspondence
  - Braiding of 4 Majorana zero modes
- Summary
- Additional Research

MFs in Particle Physics


Enrico Fermi

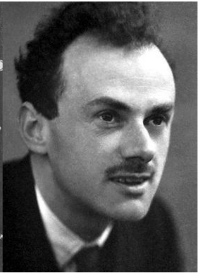
Paul Dirac


Ettore Majorana

- Fermions
  - Dirac, Weyl, Majorana
  - Fermi-Dirac statistics
  - Half-odd-integer spin
- Dirac Fermions
  - Particle $\neq$ Antiparticle
  - Charged, Massive
- Weyl Fermions
  - Particle $\neq$ Antiparticle
  - Charged, Massless
- Majorana Fermions (MFs)
  - Particle $=$ Antiparticle
  - Neutral, Massive
  - SM candidates: Neutrino, Dark Matter

MFs in Particle Physics

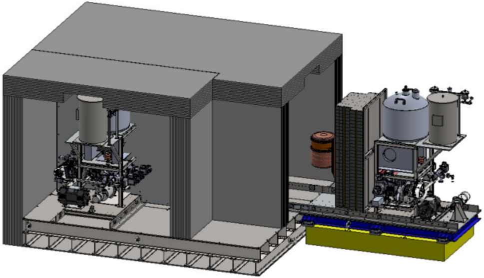

MAJORANA project:
neutrinoless double beta ($0\nu\beta\beta$) decay

- Are neutrinos MFs?
- If yes, standard model is incomplete
- Negative results for Majorana particles so far

MFs in Condensed Matter

- Superconductors (SCs)
  - Cooper pairs
    - Electron-phonon interaction pairs two electrons with opposite spin and momenta.

MFs in Condensed Matter

- Superconductors (SCs)
  - Cooper pairs
    - Electron-phonon interaction pairs two electrons with opposite spin and momenta.
  - Bogoliubov quasiparticles
    - Excitation from ground state, pairs an electron to a hole with opposite momenta.

$$H_{BdG} = \begin{bmatrix} \epsilon(k) & \Delta(k) \\ \Delta^*(k) & -\epsilon(-k) \end{bmatrix}$$

- Zero-energy excitations in *p*-wave SC may be MFs.
- Come in pairs.

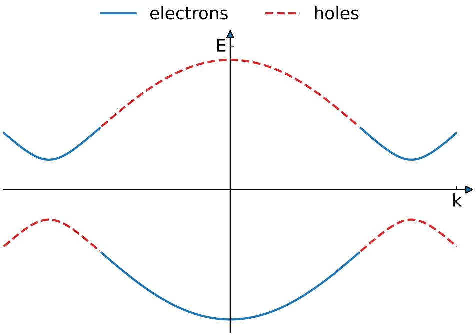

MFs in Condensed Matter

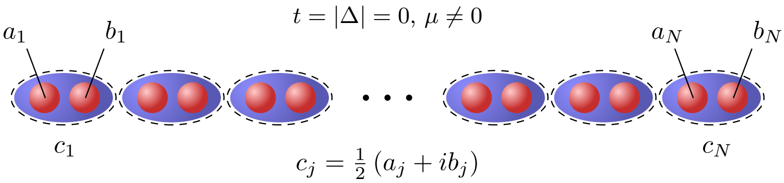

MFs in Condensed Matter

$$t = |\Delta| = 0, \; \mu \neq 0$$

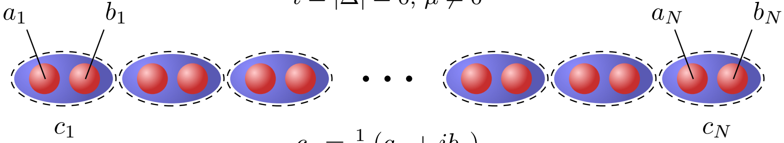

$$c_j = \tfrac{1}{2}\left(a_j + i b_j\right)$$

$$t = |\Delta| > 0, \; \mu = 0$$

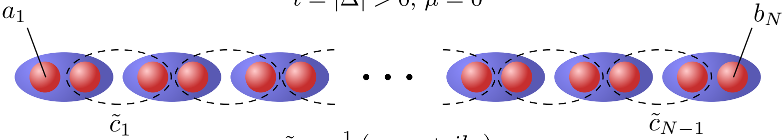

$$\tilde{c}_j = \tfrac{1}{2}\left(a_{j+1} + i b_j\right)$$

$$f = \tfrac{1}{2}\left(a_1 + i b_N\right)$$

Band Gaps and Topological Phase

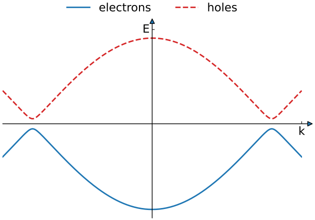

$\mu = 2.25t$

$\mathcal{M} = 1$

Trivial

Band Gaps and Topological Phase

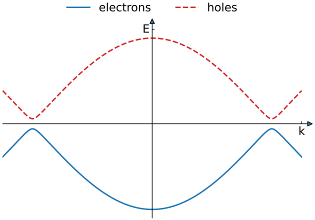

$\mu = 2.25t$

$\mathcal{M} = 1$

Trivial

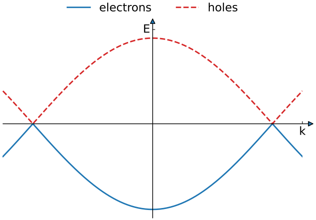

$\mu_c = 2t$

Band Gaps and Topological Phase

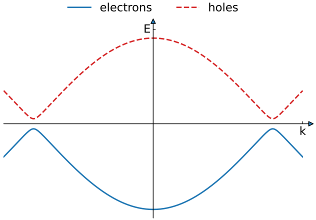

$\mu = 2.25t$

$\mathcal{M} = 1$

Trivial

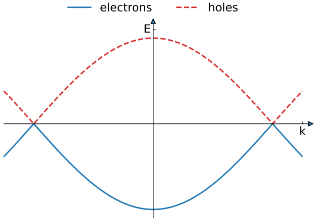

$\mu_c = 2t$

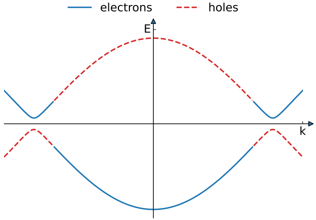

$\mu = 1.75t$

$\mathcal{M} = -1$

Non-trivial

Band Gaps and Topological Phase

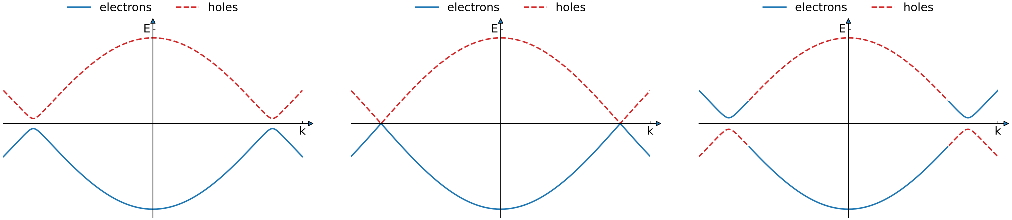

$\mu = 2.25t$ | $\mu_c = 2t$ | $\mu = 1.75t$

$\mathcal{M} = 1$ | | $\mathcal{M} = -1$

Trivial | | Non-trivial

Non-trivial phase

Large band gap $\rightarrow$ Robust against local errors $\rightarrow$ Topologically protected

Majorana Number & Bulk-Edge Correspondence

Transform to Majorana basis

$$A = -iU\mathcal{H}U^{\dagger} \tag{1}$$

Majorana number

$$\mathcal{M} = \mathrm{sgn}[\mathrm{Pf}(A)] \tag{2}$$

- If $|\mu| > 2t$, $\mathcal{M} = +1$, trivial topology
- If $|\mu| < 2t$, $\mathcal{M} = -1$, non-trivial topology

Majorana Number & Bulk-Edge Correspondence

Transform to Majorana basis

$$A = -iU\mathcal{H}U^{\dagger} \tag{1}$$

Majorana number

$$\mathcal{M} = \mathrm{sgn}[\mathrm{Pf}(A)] \tag{2}$$

- If $|\mu| > 2t$, $\mathcal{M} = +1$, trivial topology
- If $|\mu| < 2t$, $\mathcal{M} = -1$, non-trivial topology

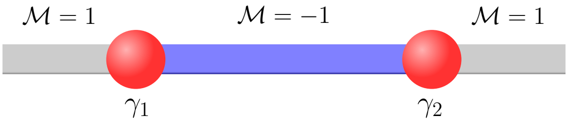

MFs in Condensed Matter

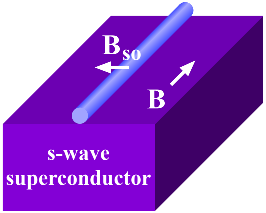

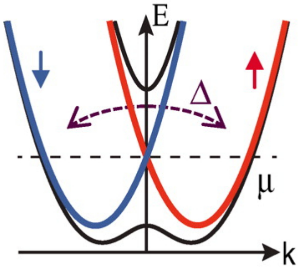

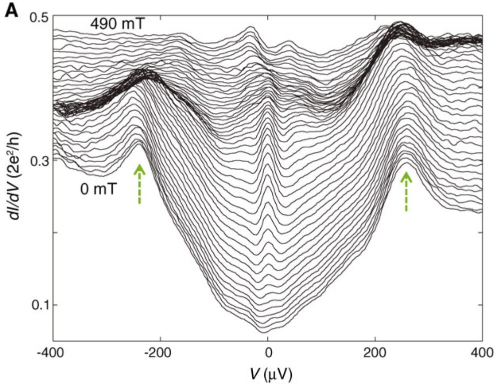

Mourik et al., *Science* **336**, 1003 (2012).

MFs in Condensed Matter

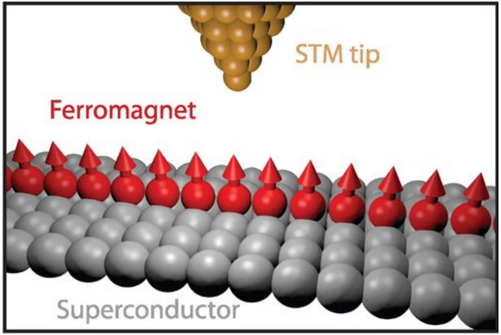

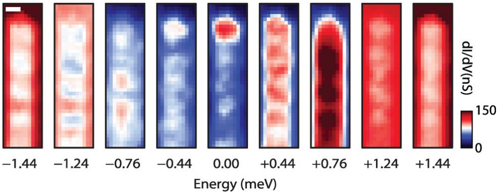

Nadj-Perge et al., *Science* **346**, 602 (2014).

MFs in Condensed Matter

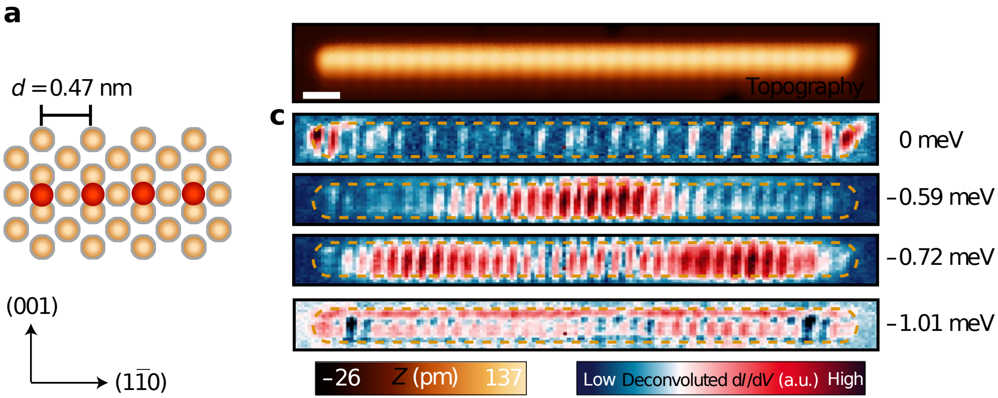

Mn atoms (red spheres) on top of superconducting Nb (brown spheres).
Schneider et al., *Nature Nanotechnology* **17**, 384 (2022).

Braiding in 2D p-wave SC

- 2D p-wave (triplet pairing) SC can exhibit half-quantum vortices.

Braiding in 2D *p*-wave SC

- 2D *p*-wave (triplet pairing) SC can exhibit half-quantum vortices.
- Allows for MF states to accumulate $e^{i\theta/2}$ phase.

Braiding in 2D *p*-wave SC

- 2D *p*-wave (triplet pairing) SC can exhibit half-quantum vortices.
- Allows for MF states to accumulate $e^{i\theta/2}$ phase.
- Braiding demonstrates non-Abelian statistics i.e. $A * B \neq B * A$,
  - $\rightarrow$ Allows for a universal quantum computer.

Braiding in 2D *p*-wave SC

- 2D *p*-wave (triplet pairing) SC can exhibit half-quantum vortices.
- Allows for MF states to accumulate $e^{i\theta/2}$ phase.
- Braiding demonstrates non-Abelian statistics i.e. $A * B \neq B * A$,
  - $\rightarrow$ Allows for a universal quantum computer.
- Combine with MFs topological protection,
  - $\rightarrow$ Fewer qubits or operations required compared to modern qubits.

Braiding in a Topological Quantum Computer

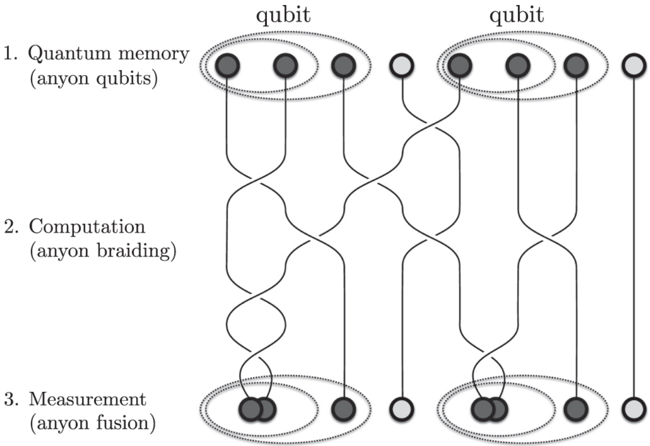

Field et. al., *Quantum Sci. Technol.* **3**, 045004 (2018).

T-junction as a Quantum Logic Gate

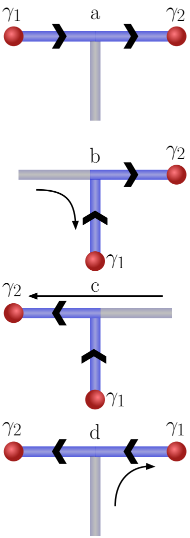

- Take pairing term $|\Delta|e^{i\phi}c_jc_{j+1}$ such that the site indices:
- Increase moving $\rightarrow$ / $\uparrow$ in the horizontal/vertical wires: $\phi = 0$,
- Decrease moving $\leftarrow$ / $\downarrow$ in the horizontal/vertical wires: $\phi = \pi$.

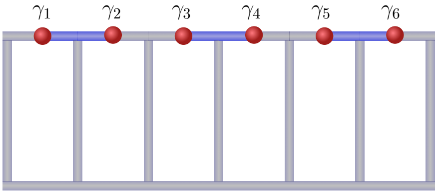

Alicea et al., *Nature Phys.* **7**, 412 (2011)

Triangular Structures for Braiding

- Consider triangular islands, topologically similar to T-junctions.
- Islands of three-fold rotational symmetry occur naturally in epitaxial growth on close-packed metal surfaces.
- Make a smooth connection from 1D to 2D superconductors.

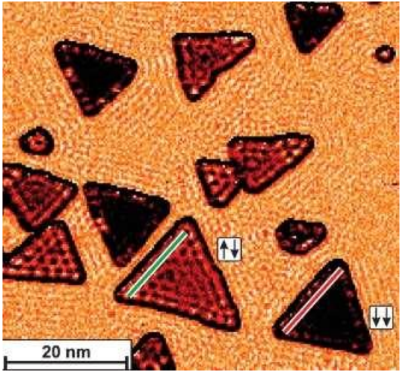

Triangular Co islands on Cu(111).
Pietzsch et al., *PRL* **96**, 237203 (2006)

Topological phase transition induced by a supercurrent

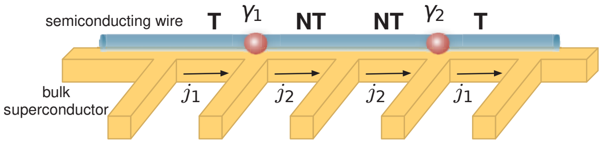

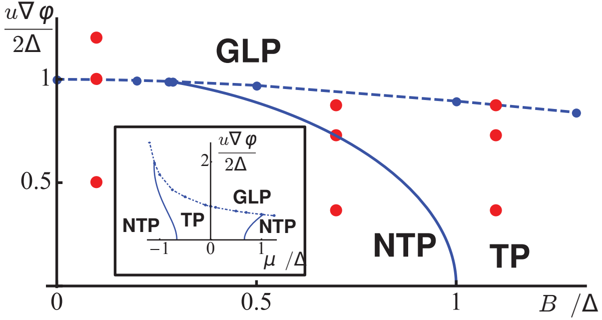

Romito et al., *PRB* **85**, 020502(R) (2012).

Topological phase transition induced by a supercurrent

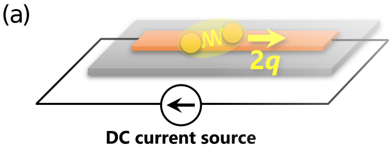

Takasan et al., *PRB* **106**, 014508 (2022).

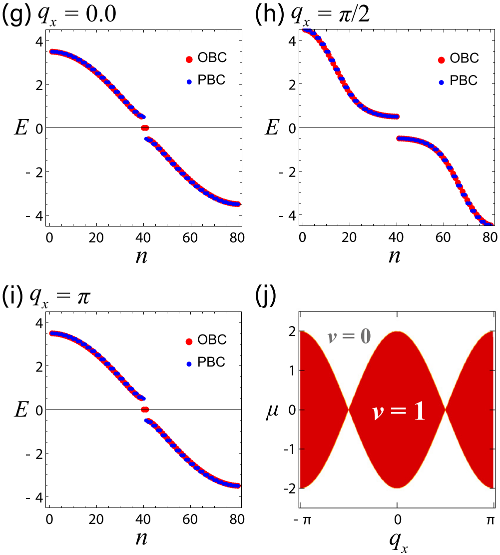

Two Proposals

- Exactly solvable "Kitaev Triangle"
  - Three fermion sites
  - Three edges controlled by Peierls phase

Two Proposals

- Exactly solvable "Kitaev Triangle"
  - Three fermion sites
  - Three edges controlled by Peierls phase
- Finite-size triangle with hollow interior
  - Under uniform vector potential
  - Bulk-edge correspondence

Kitaev Triangle

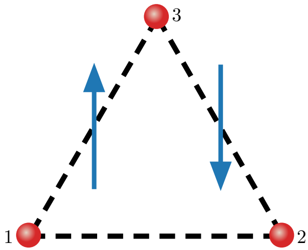

$$\mathbf{A} = [1 - 2\Theta(x)]\,\frac{2\pi}{3\sqrt{3}}\hat{\mathbf{y}} \tag{3}$$

Kitaev Triangle

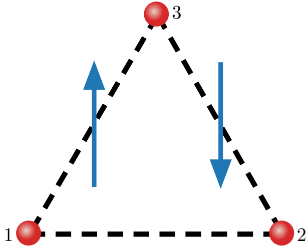

$$\mathbf{A} = [1 - 2\Theta(x)]\,\frac{2\pi}{3\sqrt{3}}\hat{\mathbf{y}} \tag{3}$$

$$\begin{aligned} c_j^\dagger c_l &\to c_j^\dagger c_l \exp\left(\frac{ie}{\hbar}\int_{r_j}^{r_l} \mathbf{A}\cdot d\mathbf{l}\right) \\ &\to c_j^\dagger c_l e^{i\phi_{jl}} \end{aligned} \tag{4}$$

$$\mathcal{H} = \sum_{\langle j,l\rangle} (-t e^{i\phi_{jl}} c_j^\dagger c_l + \Delta c_j^\dagger c_l^\dagger + h.c.) - \mu c_j^\dagger c_j \tag{5}$$

Kitaev Triangle

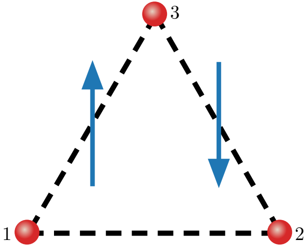

$$\mathbf{A} = [1 - 2\Theta(x)]\,\frac{2\pi}{3\sqrt{3}}\hat{\mathbf{y}} \tag{3}$$

$$\begin{aligned} c_j^\dagger c_l &\to c_j^\dagger c_l \exp\left(\frac{ie}{\hbar}\int_{r_j}^{r_l}\mathbf{A}\cdot d\mathbf{l}\right) \\ &\to c_j^\dagger c_l e^{i\phi_{jl}} \end{aligned} \tag{4}$$

$$\mathcal{H} = \sum_{\langle j,l\rangle}(-te^{i\phi_{jl}}c_j^\dagger c_l + \Delta c_j^\dagger c_l^\dagger + h.c.) - \mu c_j^\dagger c_j \tag{5}$$

In Kitaev limit, $t = \Delta \neq 0$ and $\mu = 0$,

$$(\phi_{12}, \phi_{23}, \phi_{31}) = (0, -\tfrac{\pi}{3}, -\tfrac{\pi}{3}) = \boldsymbol{\phi}_1 \tag{6}$$

MZMs localized at sites 1 and 2

Kitaev Triangle Braiding

A closed parameter path linearly interpolated between the following sets of ϕ_{jk}:

$$(\phi_{12}, \phi_{23}, \phi_{31}) : \boldsymbol{\phi}_1 \rightarrow \boldsymbol{\phi}_2 \rightarrow \boldsymbol{\phi}_3 \rightarrow \boldsymbol{\phi}_1 \tag{7}$$

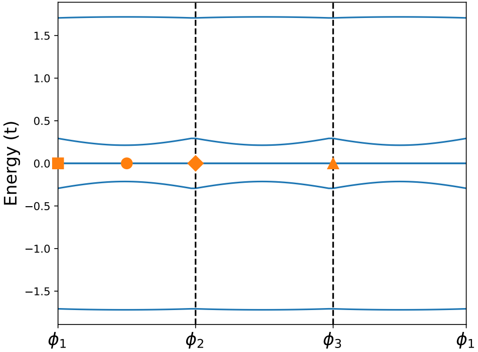

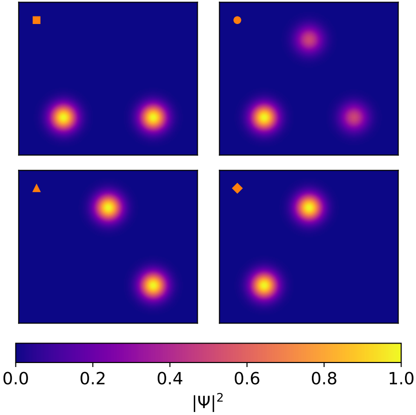

Triangular Ribbon and Topological Phases

$$\phi_{jl} = \frac{e}{\hbar}\int_{\mathbf{r}_j}^{\mathbf{r}_l} \mathbf{A}\cdot d\mathbf{l} = \mathbf{A}\cdot\mathbf{r}_{jl} = -\phi_{lj}$$

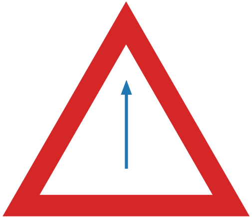

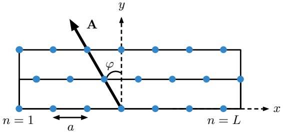

Triangular Ribbon and Topological Phases

$$\phi_{jl} = \frac{e}{\hbar}\int_{\mathbf{r}_j}^{\mathbf{r}_l} \mathbf{A}\cdot d\mathbf{l} = \mathbf{A}\cdot\mathbf{r}_{jl} = -\phi_{lj}$$

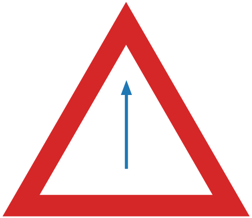

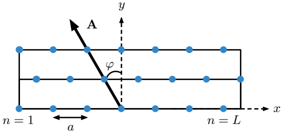

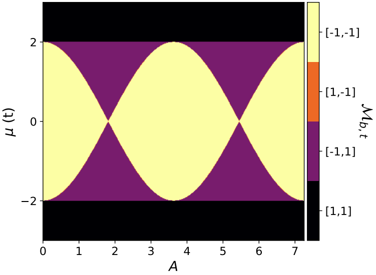

Triangular Ribbon and Topological Phases

$$\phi_{jl} = \frac{e}{\hbar}\int_{\mathbf{r}_j}^{\mathbf{r}_l} \mathbf{A}\cdot d\mathbf{l} = \mathbf{A}\cdot\mathbf{r}_{jl} = -\phi_{lj}$$

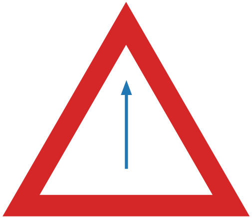

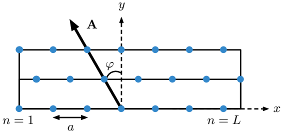

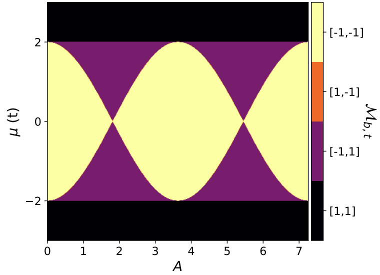

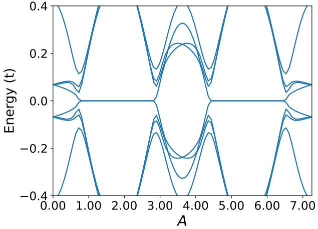

Rotating MFs on a Triangular Chain (W=1)

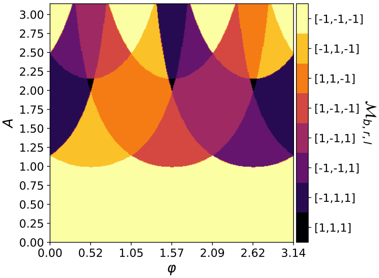

Rotating MFs on a Triangular Chain (W=1)

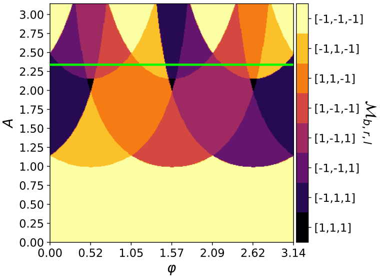

Rotating MFs on a Triangular Chain (W=1)

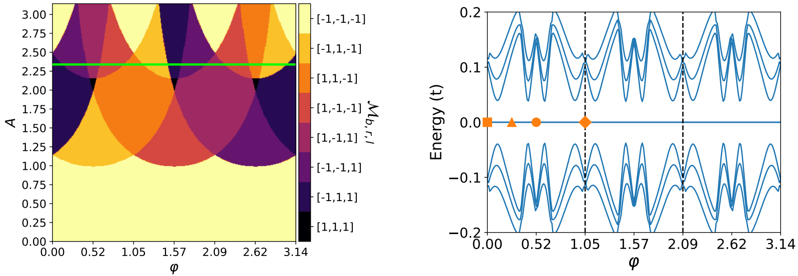

$$L = 50,\ W = 1,\ \mu = 1.1,\ A = 2.35$$

Rotating MFs on a Triangular Chain (W=1)

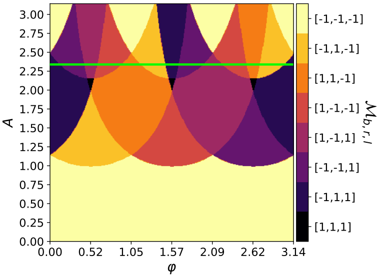

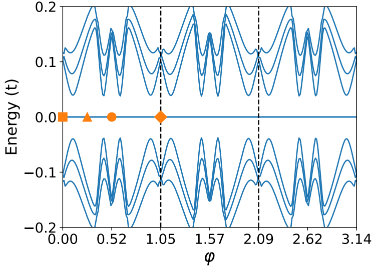

$$L = 50,\ W = 1,\ \mu = 1.1,\ A = 2.35$$

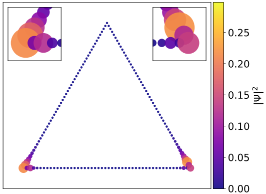

Rotating MFs on a Triangular Chain (W=1)

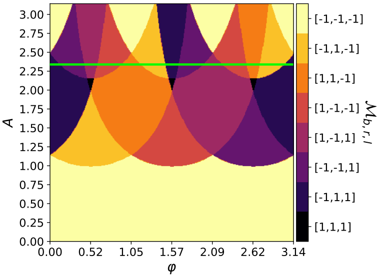

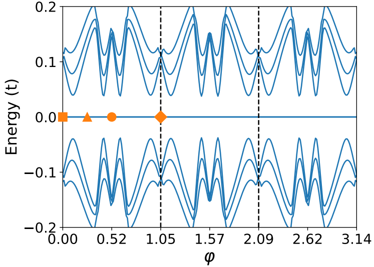

$$L = 50,\ W = 1,\ \mu = 1.1,\ A = 2.35$$

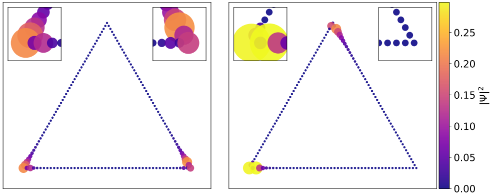

Rotating MFs on a Triangular Chain (W=1)

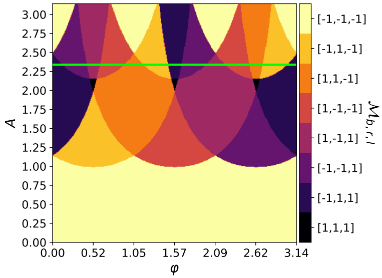

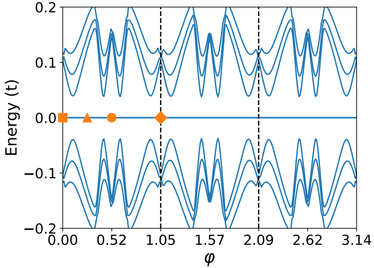

$$L = 50,\ W = 1,\ \mu = 1.1,\ A = 2.35$$

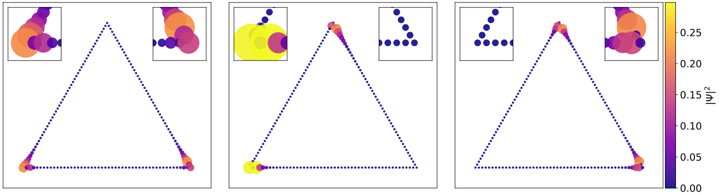

Rotating MFs on a Triangular Chain (W=1)

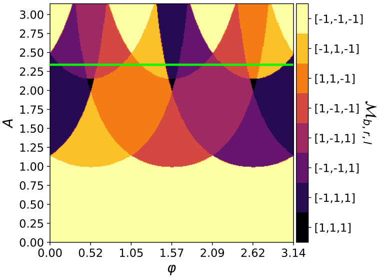

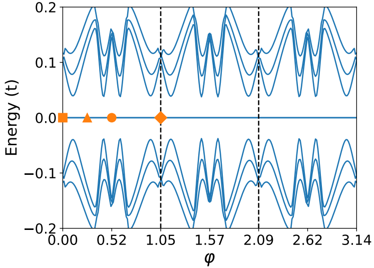

$$L = 50,\ W = 1,\ \mu = 1.1,\ A = 2.35$$

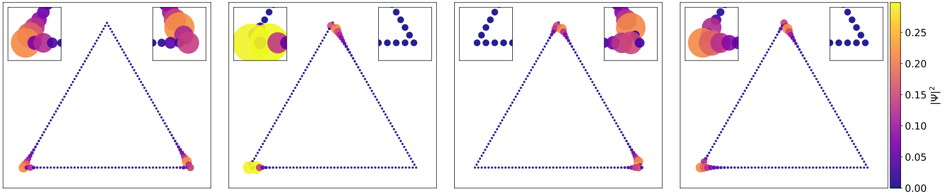

Rotating MFs on a Hollow Triangle (W=3)

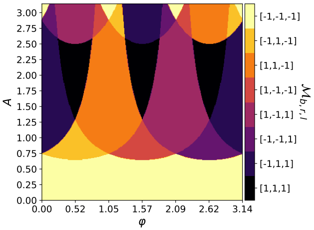

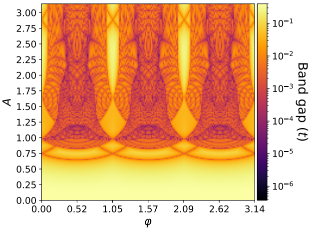

Rotating MFs on a Hollow Triangle (W=3)

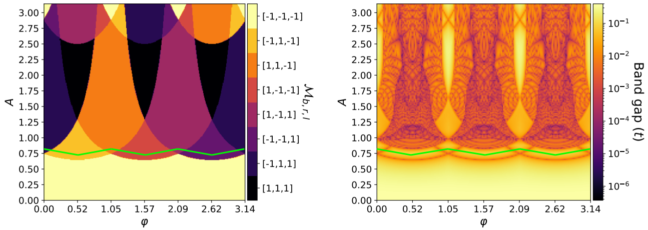

Rotating MFs on a Hollow Triangle (W=3)

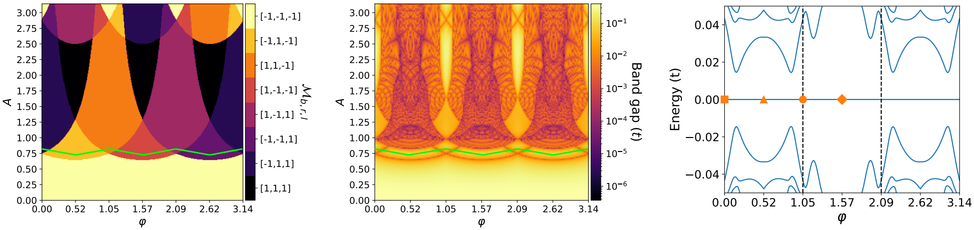

$$L = 80,\ W = 3,\ \mu = 1.6,\ (A, \varphi) = (0.83, 0) \to (0.77, \tfrac{\pi}{6}) \to (0.83, \tfrac{\pi}{3}) \to (0.77, \tfrac{\pi}{2})\ldots$$

Rotating MFs on a Hollow Triangle (W=3)

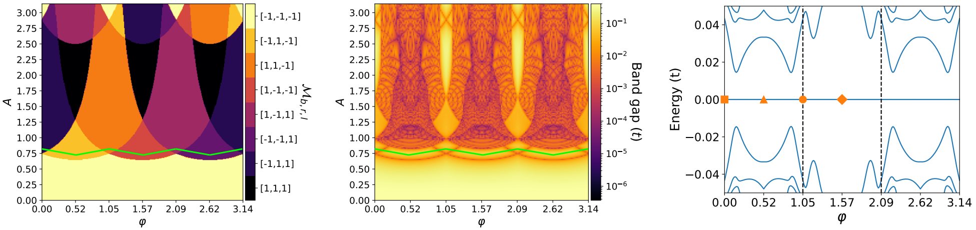

$$L = 80,\ W = 3,\ \mu = 1.6,\ (A, \varphi) = (0.83, 0) \rightarrow (0.77, \tfrac{\pi}{6}) \rightarrow (0.83, \tfrac{\pi}{3}) \rightarrow (0.77, \tfrac{\pi}{2}) \ldots$$

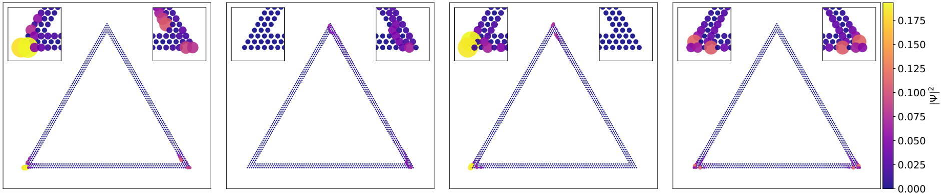

Braiding Two of Four MFs

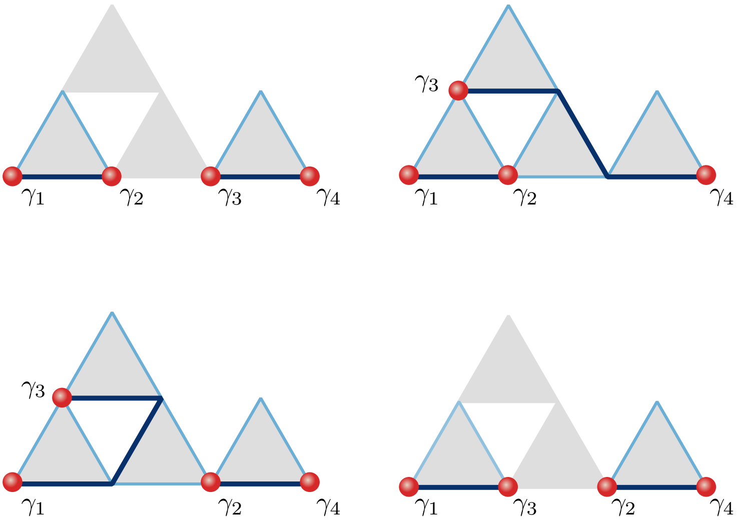

Summary

- Introduction of Peierls phase allows for a minimal Kitaev triangle, reducing fermionic sites down to 3.
- Gauge potential field and its rotation allows additional tunability of topology.
- MFs can be hosted and braided on a network of triangular islands.

Theory and Experiment

PRL **112,** 156801 (2014) PHYSICAL REVIEW LETTERS week ending 18 APRIL 2014

Floquet Fractional Chern Insulators

Adolfo G. Grushin,[1,2] Álvaro Gómez-León,[2] and Titus Neupert[3]
[1]*Max-Planck-Institut für Physik komplexer Systeme, 01187 Dresden, Germany*
[2]*Instituto de Ciencia de Materiales de Madrid, CSIC, Cantoblanco, E-28049 Madrid, Spain*
[3]*Princeton Center for Theoretical Science, Princeton University, Princeton, New Jersey 08544, USA*
(Received 25 November 2013; published 18 April 2014)

We show theoretically that periodically driven systems with short range Hubbard interactions offer a feasible platform to experimentally realize fractional Chern insulator states. We exemplify the procedure for both the driven honeycomb and the square lattice, where we derive the effective steady state band structure of the driven system by using the Floquet theory and subsequently study the interacting system with exact numerical diagonalization. The fractional Chern insulator state equivalent to the $1/3$ Laughlin state appears at $7/12$ total filling ($1/6$ filling of the upper band). The state also features spontaneous ferromagnetism and is thus an example of the spontaneous breaking of a continuous symmetry along with a topological phase transition. We discuss light-driven graphene and shaken optical lattices as possible experimental systems that can realize such a state.

PHYSICAL REVIEW LETTERS **121,** 036801 (2018)

Many-Body Dynamics and Gap Opening in Interacting Periodically Driven Systems

Ervand Kandelaki and Mark S. Rudner
Niels Bohr International Academy and Center for Quantum Devices, Copenhagen University, Blegdamsvej 17, 2100 Copenhagen, Denmark
(Received 27 October 2017; published 16 July 2018)

We study transient dynamics in a two-dimensional system of interacting Dirac fermions subject to a quenched drive with circularly polarized light. In the absence of interactions, the drive opens a gap at the Dirac point in the quasienergy spectrum, inducing nontrivial band topology. We investigate the dynamics of this gap opening process, taking into account the essential role of electron-electron interactions. Crucially, scattering due to interactions (1) induces dephasing, which erases memory of the system's prequench state and yields the intrinsic timescale for gap emergence, and (2) provides a mechanism for the system to absorb energy of the drive, leading to heating which must be mitigated to ensure the success of Floquet band engineering. We characterize the gap opening process via the system's generalized spectral function and correlators probed by photoemission experiments, and we identify a parameter regime at moderate driving frequencies where a hierarchy of timescales allows a well-defined Floquet gap to be produced and studied before the deleterious effects of heating set in.

Band structure engineering and non-equilibrium dynamics in Floquet topological insulators

Mark S. Rudner[1] ✉ *and Netanel H. Lindner*[2]

Abstract | Non-equilibrium topological phenomena can be induced in quantum many-body systems using time-periodic fields (for example, by laser or microwave illumination). This Review begins with the key principles underlying Floquet band engineering, wherein such fields are used to change the topological properties of a system's single-particle spectrum. In contrast to equilibrium systems, non-trivial band structure topology in a driven many-body system does not guarantee that robust topological behaviour will be observed. In particular, periodically driven many-body systems tend to absorb energy from their driving fields and thereby tend to heat up. We survey various strategies for overcoming this challenge of heating and for obtaining new topological phenomena in this non-equilibrium setting. We describe how drive-induced topological edge states can be probed in the regime of mesoscopic transport, and three routes for observing topological phenomena beyond the mesoscopic regime: long-lived transient dynamics and prethermalization, disorder-induced many-body localization, and engineered couplings to external baths. We discuss the types of phenomena that can be explored in each of the regimes covered, and their experimental realizations in solid-state, cold atomic, and photonic systems.

Floquet–Bloch manipulation of the Dirac gap in a topological antiferromagnet

Received: 23 October 2023

Accepted: 13 December 2024

Published online: 21 January 2025

Check for updates

Nina Bielinski[1,2], Rajas Chari[1], Julian May-Mann[1], Soyeun Kim[1,2,3], Jack Zwettler[1,2], Yujun Deng[4], Anuva Aishwarya[1,2], Subhajit Roychowdhury[5,6], Chandra Shekhar[5], Makoto Hashimoto[7], Donghui Lu[7], Jiaqiang Yan[8], Claudia Felser[5], Vidya Madhavan[1,2], Zhi-Xun Shen[4,9,10], Taylor L. Hughes[1] & Fahad Mahmood[1,2] ✉

Floquet–Bloch manipulation, achieved by driving a material periodically with a laser pulse, is a method that enables the engineering of electronic and magnetic phases in solids by effectively modifying the structure of their electronic bands. However, the application of Floquet–Bloch manipulation in topological magnetic systems, particularly those with inherent disorder, remains largely unexplored. Here we realize Floquet–Bloch manipulation of the Dirac surface-state mass of the topological antiferromagnet $MnBi_2Te_4$. Using time- and angle-resolved photoemission spectroscopy, we show that opposite helicities of mid-infrared circularly polarized light result in substantially different Dirac mass gaps in the antiferromagnetic phase, despite the equilibrium Dirac cone being massless. We explain our findings in terms of a Dirac fermion with a random mass. Our results underscore Floquet–Bloch manipulation as a powerful tool for controlling topology, even in the presence of disorder, and for uncovering properties of materials that may elude conventional probes.

Experimental Findings

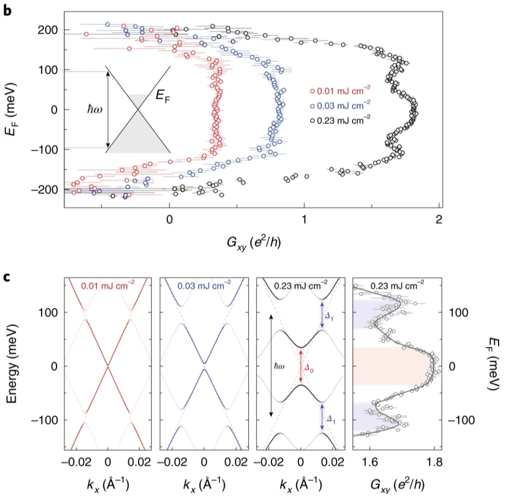

McIver et. al., *Nature Phys.* **16**, 38 (2020)

Inhomogeneous laser light on 2D systems

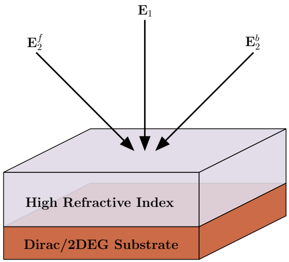

Generalized electric field at substrate surface

$$\mathbf{E}_1 = E\cos(a\omega t)\hat{\mathbf{x}},$$
$$\mathbf{E}_2 = \mathbf{E}_2^f + \mathbf{E}_2^b = -E\cos(Kx)\sin(b\omega t)\hat{\mathbf{y}}$$

where

$$K = \frac{\omega\sin(\theta_i)}{v_p} \tag{8}$$

Dirac Systems

$$\mathcal{H}(t) = v_F \boldsymbol{\sigma} \cdot (\mathbf{p} + e\mathbf{A}(t)) \tag{9}$$

$$\begin{aligned} \mathbf{E}_1 &= E\cos{(\omega t)}\hat{\mathbf{x}}, \\ \mathbf{E}_2 &= E\sin{(Kx)}\sin{(2\omega t)}\hat{\mathbf{y}} \end{aligned} \tag{10}$$

Perform Fourier time-transform, HF expansion, and the limit $Kx \ll 1$

$$\mathcal{H}^D_{\text{eff}} = v_F\sigma_x p_x + v_F\sigma_y\left(Cp_y + eB^D x\right), \tag{11}$$

where $C = 1 - \left(\frac{v_F eE}{\hbar\omega^2}\right)^2$ and

$$B^D = \frac{Kv_F^2 e^2 E^3}{4\hbar^2\omega^5}, \tag{12}$$

(13)

2DEG Systems

$$\mathcal{H}(t) = \frac{1}{2m^*}(\mathbf{p} + e\mathbf{A}(t))^2 \tag{14}$$

$$\begin{aligned} \mathbf{E}_1 &= E\cos(\omega t)\hat{\mathbf{x}}, \\ \mathbf{E}_2 &= -E\cos(Kx)\sin(\omega t)\hat{\mathbf{y}} \end{aligned} \tag{15}$$

Perform Fourier time-transform, HF expansion, apply periodic potential $V(x)$, and the limit $Kx \ll 1$

$$\mathcal{H}_{\text{eff}}^{\text{2DEG}} = \frac{1}{2m^*}\left[p_x^2 + \left(p_y - eB^{\text{2DEG}}x\right)^2\right], \tag{16}$$

where

$$B^{\text{2DEG}} = \frac{K^2 eE^2}{m^*\omega^3}, \tag{17}$$

$$\tag{18}$$

Results: Dirac Effective Magnetic Field and Quasienergies

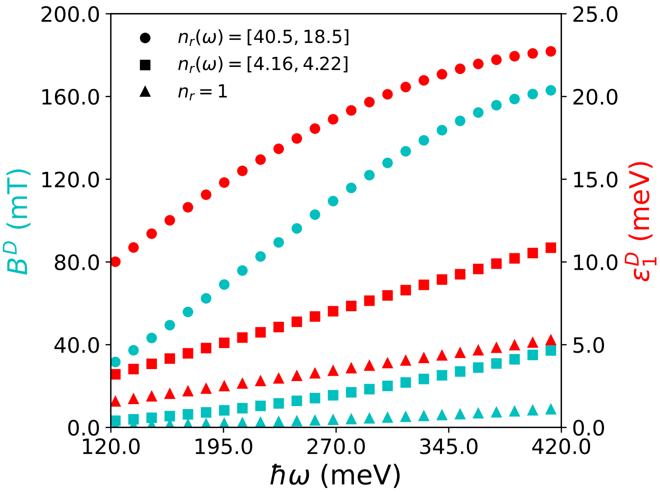

Results: 2DEG Effective Magnetic Field and Quasienergies

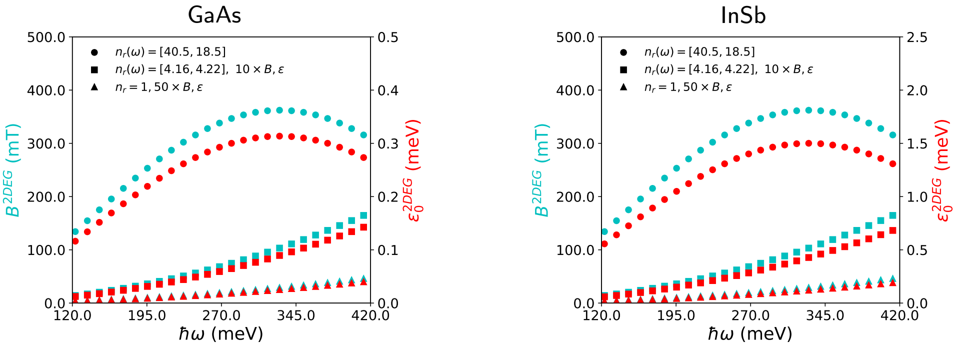

Summary

- Oblique, circularly polarized light induces QHE in Dirac and 2DEG systems.
- Showed a non-equilibrium system exhibits equilibrium results.
- Effective magnetic field can be enhanced by several parameters.

Acknowledgments

- Advisor: Dr. Hua Chen
- Committee: Dr. Martin Gelfand, Dr. Richard Eykholt, Dr. Olivier Pinaud
- Informative Discussions: Chris Ard and Muhammad Tahir
- Friends and Family
- CSU Mental Health Services

Additional results from Schneider et al.

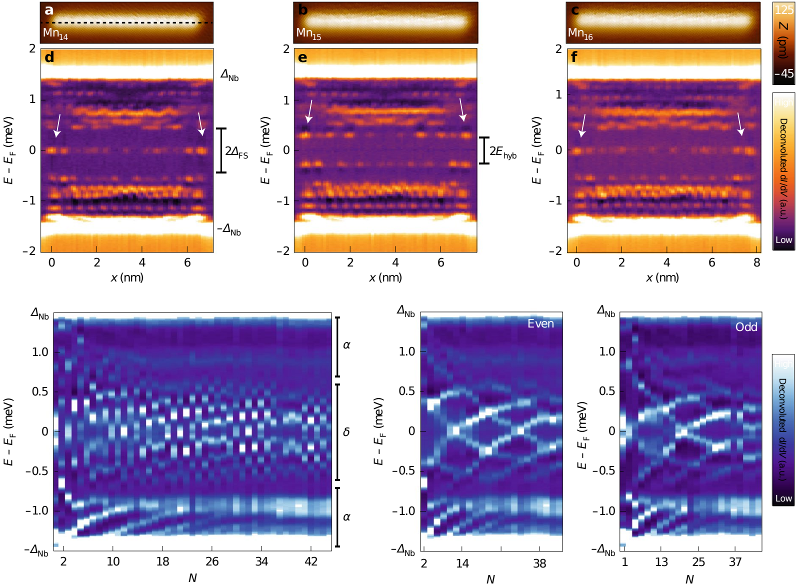

Majorana fermion notation and coupling isolation

The complex fermion operator can be written as a superposition of two Majorana fermions $c_j = \frac{1}{2}(a_j + ib_j)$. Due to the nature of Majorana fermions, $a_j^\dagger = a_j$, the creation operator is $c_j^\dagger = \frac{1}{2}(a_j - ib_j)$.

$$H = -\frac{i\mu}{4}\sum_j (a_j b_j - b_j a_j) - \frac{i}{4}\sum_{<j,l>}[(t\sin\phi - \Delta\sin\theta)a_l a_j + (t\sin\phi + \Delta\sin\theta)b_l b_j \\ +(t\cos\phi + \Delta\cos\theta)a_l b_j - (t\cos\phi - \Delta\cos\theta)b_l a_j].$$

$$(t\sin\phi_{j,l} - \Delta\sin\theta_{j,l})a_l a_j, \quad (19)$$
$$(t\sin\phi_{j,l} + \Delta\sin\theta_{j,l})b_l b_j, \quad (20)$$
$$(t\cos\phi_{j,l} + \Delta\cos\theta_{j,l})a_l b_j, \quad (21)$$
$$(t\cos\phi_{j,l} - \Delta\cos\theta_{j,l})b_l a_j \quad (22)$$

Dirac Systems

$$\mathcal{H}(t) = v_F \boldsymbol{\sigma} \cdot (\mathbf{p} + e\mathbf{A}(t)) \tag{23}$$

$$\begin{aligned} \mathbf{E}_1 &= E\cos(\omega t)\hat{\mathbf{x}}, \\ \mathbf{E}_2 &= E\sin(Kx)\sin(2\omega t)\hat{\mathbf{y}} \end{aligned} \tag{24}$$

Perform Fourier time-transform, HF expansion, and the limit $Kx \ll 1$

$$\mathcal{H}_{\text{eff}}^D = v_F \sigma_x p_x + v_F \sigma_y \left(C p_y + e B^D x \right), \tag{25}$$

where $C = 1 - \left(\frac{v_F e E}{\hbar \omega^2}\right)^2$ and

$$B^D = \frac{K v_F^2 e^2 E^3}{4\hbar^2 \omega^5}, \tag{26}$$

$$\epsilon_n^D = \pm v_F^2 \sqrt{\frac{nKe^3E^3}{2\hbar\omega^5}} \tag{27}$$

2DEG Systems

$$\mathcal{H}(t) = \frac{1}{2m^*}(\mathbf{p} + e\mathbf{A}(t))^2 \tag{28}$$

$$\begin{aligned} \mathbf{E}_1 &= E\cos(\omega t)\hat{\mathbf{x}}, \\ \mathbf{E}_2 &= -E\cos(Kx)\sin(\omega t)\hat{\mathbf{y}} \end{aligned} \tag{29}$$

Perform Fourier time-transform, HF expansion, apply periodic potential $V(x)$, and the limit $Kx \ll 1$

$$\mathcal{H}_{\text{eff}}^{\text{2DEG}} = \frac{1}{2m^*}\left[p_x^2 + \left(p_y - eB^{\text{2DEG}}x\right)^2\right], \tag{30}$$

where

$$B^{\text{2DEG}} = \frac{K^2 eE^2}{m^*\omega^3}, \tag{31}$$

$$\epsilon_n^{\text{2DEG}} = \frac{\hbar K^2 e^2 E^2}{m^{*2}\omega^3}\left(n + \frac{1}{2}\right) \tag{32}$$